Geminate recombination and relaxation of molecular iodine

N. Alan AbulHaj and David F. Kelley

Citation: The Journal of Chemical Physics **84**, 1335 (1986); doi: 10.1063/1.450843
View online: http://dx.doi.org/10.1063/1.450843
View Table of Contents: http://scitation.aip.org/content/aip/journal/jcp/84/3?ver=pdfcov
Published by the AIP Publishing

Geminate recombination and relaxation of molecular iodine

N. Alan Abul-Haj and David F. Kelley[a),b),c)]
Department of Chemistry, University of California, Los Angeles, California 90024
and Department of Chemistry,[d)] Colorado State University, Fort Collins, Colorado 80523

(Received 20 August 1985; accepted 25 October 1985)

Picosecond absorption kinetics of I_2 in several room temperature solvents have been obtained. Probe wavelengths of 500, 580, and 640 nm were used following excitation with 30 ps pulses of 532, 630, or 683 nm light. The results indicate that population of the electronically excited $A(^3\pi_{1u})$ and $A'(^3\pi_{2u})$ states occurs rapidly (<30 ps) following dissociation. Analysis of transient absorption intensities indicates that repopulation of the ground electronic state requires about 30–50 ps. We propose that the difference in population times may be understood in terms of trapping in weakly bound electronic states (perhaps $^3\pi_{0^-u}$) which relax to populate the ground electronic state, or in terms of slow atom recombination into the ground state. The results show that for I_2 in CCl_4, X state repopulation and vibrational relaxation occur on roughly comparable time scales. The results also show that the recombination dynamics are determined primarily by the nature of dissociative state, not the recoil energy. Vibrational relaxation rates through the ground state mainfold were interpreted in terms of vibration to translation energy transfer as given by the Schwartz, Slawsky, Herzfeld theory. This was found to work quite well for weakly interacting solvents such as $CFCl_3$, $C_2Cl_3F_3$, and CCl_4. This simple theory breaks down for more strongly interacting solvents such as CH_2Cl_2 and $CHCl_3$.

INTRODUCTION

The photodissociation and recombination of condensed phase molecular halogens are among the most extensively studied of all chemical reactions. I_2 or Br_2 dissolved in inert solvents may be dissociated by absorption of visible light. The nascent atoms are held in close proximity to each other by the surrounding solvent cage, thereby greatly enhancing the probability of geminate recombination. The relatively low reactivity of bromine and especially iodine atoms eliminates the problems of other chemical reactions taking place. This fact, along with well understood spectroscopy of I_2 and Br_2 makes these systems ideal for recombination and relaxation studies.

Inspection of the relevant potential curves[1] reveals that following dissociation, recombination may result in molecules which are formed in electronically and/or vibrationally excited states (see Fig. 1). The dynamics following photoexcitation therefore consist of several different processes. These include direct dissociation or predissociation, solvent cage induced atom recombination, as well as vibrational and electronic relaxation.

The solvent cage effect was first discussed in the context of I_2 by Rabinowitch and Wood[2] and later in a series of papers by Noyes *et al.*[3] These and more recent papers[4,5] have shown that the fraction of iodine atoms which escape the cage is related to viscosity and density of the solvent. These studies describe the net effect of the solvent cage, but provide very little information about the actual recombination and relaxation dynamics.

The first experiments to study these reaction dynamics by time resolved spectroscopy were done by Eisenthal *et al.*[6] In these experiments dilute solutions of I_2 in CCl_4 and hexadecane were excited at 530 nm which is close to the static absorption maximum. Excitation at this wavelength predominately populates the upper vibrational levels of the $B(^3\pi_0)$ state which rapidly predissociates to ground state iodine atoms.[1,7] The intense 530 nm, 6 ps excitation laser pulses used in these experiments excited a significant fraction of the

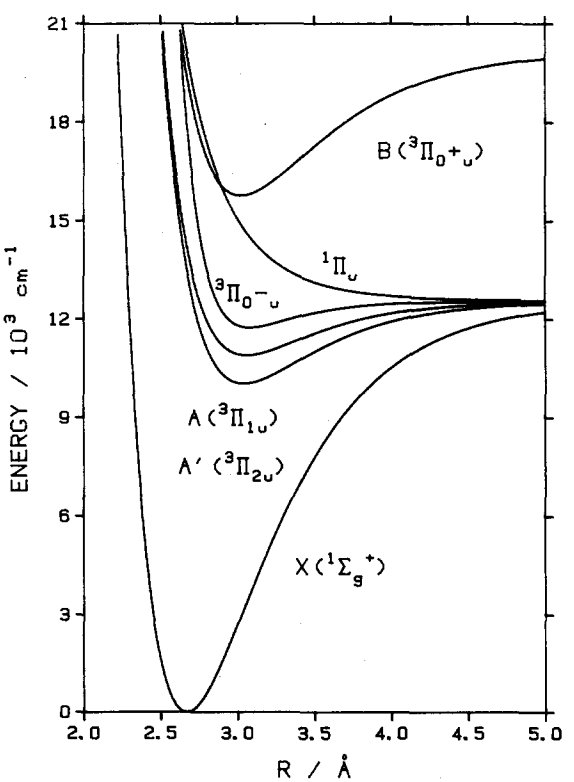

FIG. 1. Approximate gas phase potential energy curves for several of the relevant electronic states of molecular iodine. These curves are based upon Morse potentials, and are inaccurate at large internuclear separations.

[a)] Alfred P. Sloan Fellow.
[b)] IBM Faculty Development Award Recipient.
[c)] Author to whom correspondence should be addressed.
[d)] Present address of D.F.K.

 0021-9606/86/031335-10$02.10

ground state molecules, resulting in a reduced transient absorption or "bleach". The recovery of this ground state bleach was subsequently monitored by 530 nm and 6 ps probe pulses. Ground state repopulation times of 70 and 140 ps in hexadecane and CCl_4 solvents respectively, were reported. Similar studies have been performed in other hydrocarbons[8] and in liquid xenon[9] and comparable bleach recovery times (60–100 ps) were reported. This 100 ps time scale was interpreted as the time required for geminate recombination of the atoms. However, subsequent trajectory,[10–13] generalized Langevin[14–16] and diffusion[17] calculations predicted much shorter time scales. Nesbitt and Hynes[18] therefore suggested that relaxation through the ground state vibrational manifold, not recombination, was the step limiting the rate of ground vibronic state repopulation. Molecular dynamics calculations by Wilson *et al.*[10] as well as generalized Langevin equation calculations by Adelman[16] also indicated that this was the case. These calculations indicated that vibrational relaxation should take place on the 100 ps to 1 ns time scale. Furthermore, Franck–Condon calculations indicate that the $B \leftarrow X$ absorption will be significantly shifted to the red for vibrationally unrelaxed molecules. The extent of this shift depends upon the level of vibrational excitation. Picosecond spectroscopic studies by Wilson[10,19] reported transient absorptions in the red and near infrared regions. The absorption kinetics were also consistent with this explanation.

Shortly thereafter, Flynn *et al.*[20,21] published fluorescence results that indicated that recombination in low temperature rare gas matrices resulted in electronically excited $A(^3\pi_{1u})$ and $A'(^3\pi_{2u})$ states of I_2 and Br_2. Similar studies for Cl_2 had previously been reported.[22,23] These results implied that room temperature solution phase recombination into electronically excited states might also be an important relaxation pathway. Theoretical calculations by Ali and Miller[24] supported this expectation. Picosecond absorption studies of I_2 in CCl_4 and several other solvents by Kelley *et al.*[25] confirmed that a significant fraction of the molecules recombined into the A and A' states. Furthermore, it was also shown that these states have nanosecond lifetimes in chlorinated hydrocarbon solvents and that the lifetimes were solvent dependent. These studies detected a strong absorption in the 575–800 nm region that was assigned to the $A'(^3\pi_{2u})$ state. However, no time dependent spectral shifts associated with vibrationally unrelaxed ground state populations were detected. It was therefore concluded that, contrary to the calculations, vibrational relaxation takes place in < 50 ps and that much of the 140 ps bleach recovery transient was associated with the time required for atom recombination. Recently Harris *et al.*[26] has performed picosecond transient absorption experiments with better time resolution and signal to noise ratios than had been previously available. These results show weak time dependent spectral shifts in the red and near infrared spectral regions superimposed upon the A' state absorption. The spectral shifts were interpreted in terms of slow (50–100 ps) vibrational relaxation. These results indicated that at least some of the ground state recombination occurs very rapidly (< 20 ps). This result must be viewed in light of the recent theoretical results by Sceats.[27] These studies indicate that a significant fraction of the molecules may become trapped in very weakly bound electronic states such as the $^3\pi_{0^-u}$ state. Relaxation from these states may occur on the tens of picoseconds time scale and would result in slow repopulation of the ground state. The situation is made more ambiguous by the results of studies of organic radical pair geminate recombination rates and quantum yields which may be relevant to iodine atom recombination rates. Studies of the caged recombination of benzyl radicals indicate that some geminate recombination occurs on the hundreds of picosecond time scale.[28] In this paper we report picosecond transient absorption kinetics which clarify the ambiguities in the relative rates of iodine recombination, electronic, and vibrational relaxation.

EXPERIMENTAL

The experimental apparatus is shown schematically in Fig. 2. It consists of a streak-camera absorption spectrometer based on an actively/passively mode locked Nd:YAG laser with two amplifiers. In this technique the fluorescence of an organic dye is passed through the sample excitation volume and then imaged through a 0.25 m SPEX monochromator and onto a Hamamatsu C979 streak-camera. A transient absorption or bleach alters the time dependent fluorescence intensity observed by the streak camera. Comparison of apparent fluorescence kinetics with and without sample excitation yields very accurate kinetics of a 10 nm band. The temporal instrument response is determined primarily by the laser pulse width and is about 35 ps FWHM with 532 nm excitation. Deconvolution with the instrument response function permits the resolution of somewhat faster transients. This apparatus has recently been described in greater detail.[29]

Samples were excited with 3 mJ, 25 ps pulses of 532 nm light. Reduction of the excitation intensity by a factor of 50 had no effect upon the kinetics. Alternatively, some samples were excited with ~1 mJ, 20 ps pulses of 630 or 683 nm light

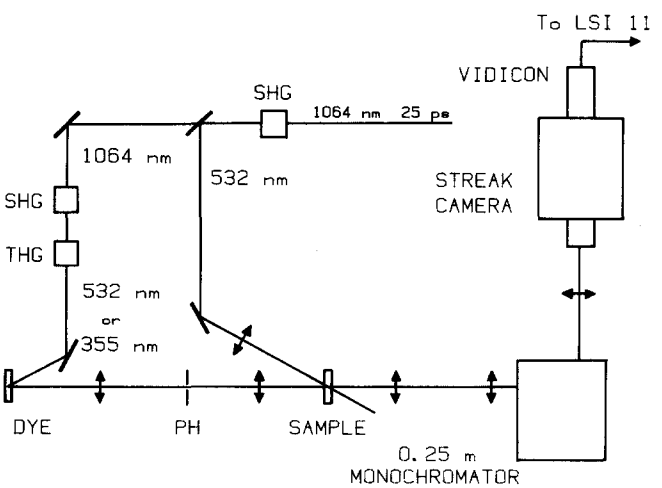

FIG. 2. Schematic diagram of the picosecond absorption spectrometer. The symbols have the following meanings: Double headed arrows; focusing lens, PH; pinhole. SHG; second harmonic generator, THG; third harmonic generator.

generated by the stimulated Raman shifting of 532 nm pulses by CH_4 or H_2, respectively. Active/passive stabilization of the laser oscillator results in 532 nm shot-to-shot stability of about $\pm$ 5%. High stability, along with very low long term (hours) drift of the laser intensity results in excellent reproducibility of total absorbance changes. This permits direct comparison of kinetics taken at different wavelengths.

Typical sample concentrations were 5 mM for 532 nm excitation experiments, and 9 mM for 630 and 683 nm excitation. Samples were degassed by 8 cycles of freeze–pump–thaw and transferred to the sample cells under dry nitrogen. This proved to be particularly important for the 630 and 683 nm excitation experiments. The effects of oxygen were negligible in CCl_4, but significant in $CHCl_3$ and especially in CH_2Cl_2 solvents. Although no results obtained in hydrocarbon solvents are reported here, we note that these solvents showed the largest oxygen effects, especially following red excitation and at high concentrations. These observations may be relevant to the interpretation of the results presented in Ref. 19. High sample concentrations (> 15 mM) can also result in significant excited state ($I_2^* + I_2$) diffusion controlled reactions. This subject will be discussed in a later paper.[30]

RESULTS AND DISCUSSION

Transient absorption kinetics and relative intensities

Transient difference kinetics (transient minus static absorption intensities) of I_2/CCl_4 solutions following 532 nm excitation are shown in Figs. 3 and 4. The 580 and 640 nm kinetics follow biphasic decays. At long times (> 250 ps) the decays are exponential, with a 2.7 ns time constant. This long lived absorption extends from 550 to > 800 nm with a wavelength independent lifetime.[25(a)] Previous studies have shown that the long lived red absorption is due to population in the $A'(^3\pi_{2u})$ state.[25(c)] This state has a depth of $\sim$2500 cm^{-1} (Ref. 1) and the 2.7 ns lifetime corresponds to about the time required for molecules in this state to achieve vibrational energies close to the dissociation limit. At these energies the Franck–Condon factors permit facile crossing to the X state potential curve[24] (see Fig. 1). The static absorption spectrum of I_2 in CCl_4 is peaked at 516 nm and has a large ($\sim$90% of the maximum) absorbance at 500 nm. The 500 nm kinetics show a negative transient or bleach indicating ground state depletion. The bleach recovery also follows biphasic kinetics, but does not recover completely on the 10 ns time scale. Extrapolation to long times (> 10 ns) indicates the presence of a slight bleach which decays on a much longer time scale. The amount of the very long lived bleach corresponds to the fraction of molecules which escape the solvent cage, and recombine on a microsecond time scale.[3] The bleach at times greater than 250 ps relaxes to this long time value with a 2.7 ns exponential decay. This is identical with the A' state lifetime observed at 580 and 640 nm. We therefore assign the 2.7 ns component of bleach recovery to ground state repopulation from the $A'(^3\pi_{2u})$ state. Curves corresponding to the 2.7 ns and very long lived decays (convolved with the instrument response function) are also shown in Figs. 3 and 4.

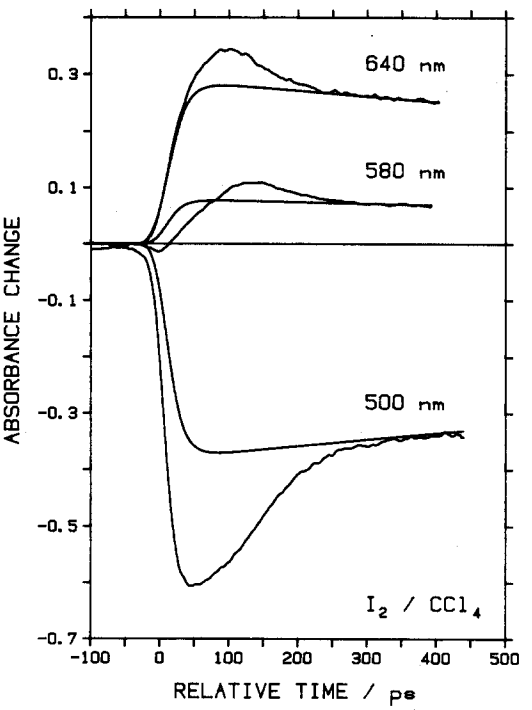

FIG. 3. Experimental transient absorption difference (transient minus static absorption intensities) kinetics of I_2 in CCl_4 at 500, 580, and 640 nm. Also shown with the 580 and 640 nm kinetics are curves calculated from the convolution of 2.7 ns exponential decays with the instrument response function. The curve shown with the 500 nm kinetics was calculated from the convolution of the instrument response function with a 2.7 ns exponential bleach recovery and a small (0.17 of the total bleach) constant bleach. The instrument response function was 35 ps full width at half-maximum.

The short time (< 250 ps) kinetics at all wavelengths are somewhat more complicated. Figure 3 shows that the majority of the 640 nm absorption is due to population in the A' state, and the appearance of this absorption follows a $\lesssim$15 ps rise time when convolved with the instrument response function. This 15 ps corresponds to the B state predissociation lifetime[6,26] and we conclude that atom recombination

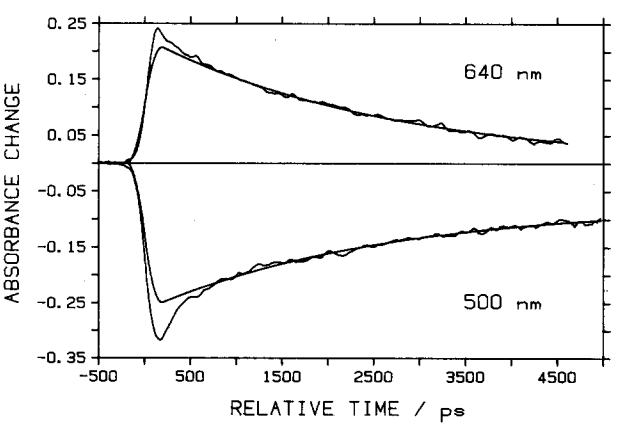

FIG. 4. Analogous plots to those in Fig. 3 except that probe wavelengths were 640 and 500 nm. The instrument response function was $\sim$180 ps FWHM on this streak rate resulting in an apparent decrease of the amplitudes of the fast transients.

into the $A'(^3\pi_{2u})$ state is very fast (<30 ps). The 580 and 640 nm kinetics also indicate the presence of short lived transients superimposed upon the A' state absorption. Calculations by Wilson[10] indicate that vibrationally unrelaxed ground state population should also absorb in the red and near infrared regions. We have performed Franck–Condon calculations from the $v = 0$–30 ground state vibrational levels to the appropriate $^1\pi_{1u}$, $B(^3\pi_0)$, and $A(^3\pi_{1u})$ excited states. These calculations used the semiclassical Airy uniform approximation.[31] They indicate that a 640 nm absorption results primarily from $v = 4$–10 population while a 580 nm absorption is from $v = 1$–5 population. We therefore assign the short lived transients to population in excited vibrational levels of the ground electronic state. These short lived transients have also been detected by Harris *et al.*,[26] but due to the low intensities compared to strong A' state absorption were not detected by earlier picosecond spectral studies.[25(a)]

The 500 nm bleach recovery kinetics also show a short lived transient which relaxes on the same time scale as the 580 and 640 nm short lived absorptions. This rapid bleach recovery component may therefore be assigned to ground vibronic state repopulation following recombination into the ground electronic state. As indicated above the X state is repopulated on the nanosecond time scale from the A' state, but this process is sufficiently slow to be unimportant in the analysis of the <250 ps kinetics. The present analysis treats this slow (nanosecond) process and rapid (<250 ps) ground state repopulation processes separately.

Figure 3 shows that the red absorptions have finite rise times and that the maximum absorbances at 580 and 640 nm occur at ~ 130 and ~ 100 ps, respectively. These kinetics imply that the fast component of bleach recovery is at least in part due to the time required for relaxation through the lower vibrational levels. We may not, however, infer from this observation that all short time scale (<250 ps) X state repopulation occurs promptly following dissociation. The relative times required for X state repopulation and vibrational relaxation may be inferred from a comparison of the intensities of the fast transients at 580 and 640 nm with that at 500 nm. The recent molecular dynamics calculations by Wilson[10] are relevant to this comparison. Wilson has calculated transient absorption spectra at various times following excitation. We emphasize that in these calculations only X state recombination was considered, and X state repopulation was very rapid. These calculations show that as vibrational relaxation proceeds the absorption maximum starts out in the near infrared, evolves toward shorter wavelengths and finally relaxes to the static absorption maximum at 526 nm. One very important finding of these calculations is that the absorption maxima at 580 or 640 nm are 50%–60% of the long time (vibrationally relaxed) absorption at 500 nm. This result is largely due to the $X \rightarrow B(^3\pi_0)$, $X \rightarrow {}^1\pi_u$, and $X \rightarrow A(^3\pi_{1u})$ Franck–Condon factors and holds irrespective of the vibrational relaxation rate. The predictions from these calculations should therefore be applicable to all weakly interacting inert solvents.

Calculation technique

We report here calculations based upon an isolated binary collision model for vibrational relaxation and semiclassical Franck–Condon factors. Calculations of transient population distributions along with Frank–Condon factors permit the determination of transient absorption spectra and kinetics which are analogous to those reported by Wilson. The calculation of the transient vibrationally unrelaxed population distributions is discussed below:

The transition probability matrix was constructed such that the $P(i,j)$ element represents the probability of an I_2^*-solvent collision inducing a transition from the jth to the ith vibrational levels. The $P(0,1)$ element of this matrix may be taken as an adjustable parameter. The remaining elements may be determined on the basis of Schwartz, Slawsky, Herzfeld (SSH)[32,33] theory. Specifically:

$$P(n, n+j) = [P(0,1)]^j (n+1)(n+2)\cdots(n+j)/(j!)^2. \quad (1)$$

The probability matrix is then constrained to obey the Onsager relations of detailed balance and completeness. Specifically:

$$1 = \Sigma_i P(i,j) \quad \text{for all } j$$

and

$$P(i,j) = P(j,i)\exp(-E_{ij}/kT),$$

where E_{ij} is the energy separation between levels j and i. Adherence to these relations requires slight modification from the values given in Eq. (1). Equation (1) assumes that all energy transfer is from the I_2 vibrations to translational (V–T) rather than to vibrational (V–V) motions of the solvent. We will comment on the validity of this assumption later.

A transient population distribution may be represented by a vector, the ith element of which is given by the population in the ith vibrational level. Multiplication of this vector by the collisional transition probability matrix simulates a single I_2–solvent collision. If the collision rate is taken to be 10^{13} s^{-1}, then ten successive multiplications simulates the evolution of the vibrational population distribution over 1 ps. Through successive multiplications transient population distributions may therefore be calculated. Convolution of these distributions with the Franck–Condon factors permits the calculation of transient absorption spectra for any time following excitation. If the initial conditions put all of the transient population immediately into the highest vibrational level (rapid X state repopulation), then this simulation should yield spectra similar to those generated by Wilson's I_2/Xe molecular dynamics calculations[10(b)] which also ignore V–V energy transfer. With the condition of rapid X state repopulation, and if $P(0,1)$ is taken to be (1/550), then we find that these calculations and Wilson's molecular dynamics calculations yield essentially identical results. With the above conditions the two sets of calculations quantitatively agree on both the intensities and kinetics of the transient absorption spectra. It is interesting to note that this value of $Z_{10} = 1/P(0,1) = 550$ differs only slightly from the value of ~ 500 determined for $I_2(v=1)$–I_2 collisions by ultrasonic absorption studies.[34]

Ground electronic state repopulation rates

In the absence of other 500 nm absorptions the maximum amplitude of the fast component of the bleach recovery

is indicative of the fraction of molecules which rapidly (<250 ps) repopulate the ground electronic state. Figure 3 shows that the rise of the 500 nm bleach is almost pulse width limited indicating that the amount of bleach is only slightly affected by a very short lived (<30 ps) transient associated with population in the B state. If all X state repopulation is assumed to be rapid, then on the basis of both ours and Wilson's calculations it is predicted that the maximum amplitudes of the vibrationally unrelaxed X state absorbances (i.e., the rapidly decaying components) obtained at 580 and 640 nm should be about 50%–60% of the amplitude of the fast component of 500 nm bleach recovery. It is further predicted that the 640 nm absorbance maximum will occur significantly after excitation and that the 580 nm absorbance maximum will occur significantly after that. We emphasize that these predications should hold only if all X state repopulation occurs rapidly compared to vibrational relaxation. However, if repopulation of the X state is slow, then population never accumulates in the excited vibrational levels. That is, if vibrational relaxation were rapid compared to X state repopulation then relaxation from the excited vibrational levels prevents the accumulation of large populations in these levels. In this case one predicts only a small "steady state" population in the excited vibrational levels while repopulation into the highest vibrational level occurs. This would result in very small excited vibrational state absorption at 580 and 640 nm that would relax at the same rate as the fast component of the bleach recovery. Furthermore, if vibrational relaxation were very rapid, then one would expect the 580 and 640 nm absorbance maxima to occur promptly following dissociation.

The experimental transient difference curves shown in Fig. 3 are due to A' state absorption, ground state depletion (due, in part, to cage escape) as well as the short lived transients associated with molecules which recombine onto the ground state surface. As indicated above, curves corresponding to the long lived transient may be generated by fitting the data at times longer than ~ 250 ps, and are also shown in Fig. 3. Comparison of the SSH theory calculations with the experimental data is facilitated by subtracting off these long lived transients. These short time "residual" absorbances generated by this subtraction are shown in Fig. 5. Also shown are curves calculated from the SSH theory dynamical simulation outlined above. These calculations ignore the possibility of absorption from the $B(^3\pi_0)$ state prior to its predissociation. It is therefore inappropriate to compare the calculated and experimental kinetic curves within the first ~ 30 ps following excitation. This is true in all solvents. The calculated curves in Fig. 5(a) assume a $v=1$ to $v=0$ transition probability [$P(0,1)$] of 1/320 per solvent collision. They further assume that the time required for X state repopulation is limited only by the ~ 15 ps lifetime for B state predissociation (i.e., all atom recombination and X state repopulation occurs rapidly following dissociation). All calculated curves have been convolved with the 35 ps FWHM instrument response function. In all cases the Z_{10} values have been chosen to give the best fit to the 500 nm data. The applicability of SSH theory, and the X state repopulation rate used in the calculation, may then be assessed by the fit of

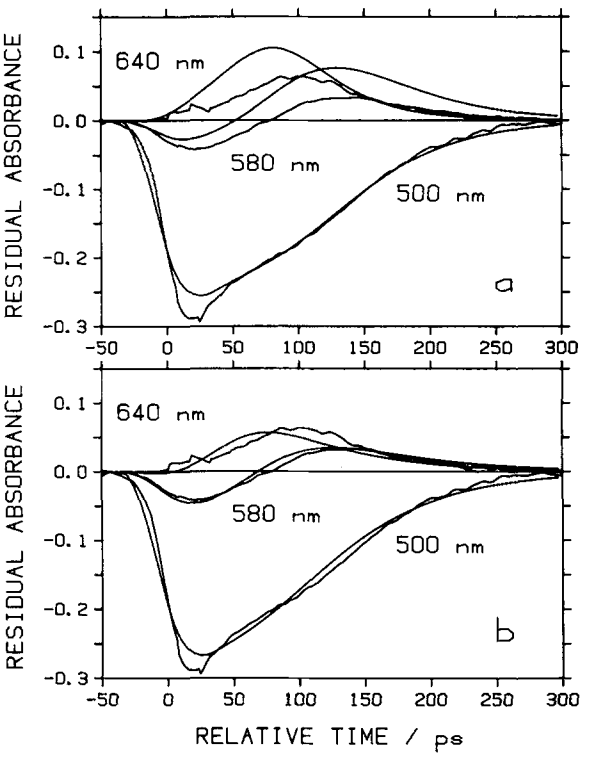

FIG. 5. Plots of short lived residual transients of I_2 in CCl_4 at 640, 580, and 500 nm vs time. Curves were constructed by subtracting the calculated from the experimental curves in Fig. 3. Also shown are curves calculated on the basis of SSH theory with (a) $Z_{10}=320$ and a rapid X state repopulation ($\tau_x=15$ ps), and (b) $Z_{10}=210$ and an X state repopulation time of 55 ps ($\tau_x=55$).

the 580 and 640 nm calculated curves. The calculated curves shown in Fig. 5(b) assume $P(0,1)=1/210$ and that X state repopulation occurs with a time constant τ_x of 55 ps. Inspection of Figs. 5(a) and 5(b) reveals that the latter calculated curves are in much better agreement with the experimental data. While the recent picosecond studies by Harris *et al.*[26] have shown that some fraction of the atoms recombine promptly following dissociation, this does not rule out the possibility of a significant fraction of the molecules repopulating the X state on the tens of picoseconds time scale. Taking account of the ~ 15 ps predissociation lifetime, the results reported here show that the average X state repopulation time is ~ 40 ps. This conclusion holds irrespective of the validity of SSH theory. For example, a relatively rapid relaxation in the lower vibrational levels compared to upper ones would result in a reduced maximum absorbance at 580 nm with an increase in the 640 nm maximum. No deviation from SSH theory could produce a reduction of the maximum transient absorption at both 580 and 640 nm. Furthermore, these results show that vibrational relaxation is relatively rapid. The average time required for a $v=1$ to $v=0$ transition is estimated to be ~ 20 ps with shorter estimates for relaxation between higher levels. Figure 5(b) shows that the 640 nm vs 580 nm maximum absorbances are in excellent agreement with the predictions of simple SSH theory (with a 55 ps X state repopulation time), indicating

that relaxation slows in the lower vibrational levels as predicted by this isolated binary collision V–T model.

The results shown in Fig. 5 imply that the I_2/CCl_4 system is intermediate between the two extremes of repopulation versus relaxation rates discussed above and that X state repopulation and vibrational relaxation occur on roughly comparable time scales. If this implication is correct, one predicts that the absorbance ratios predicted by Wilson's calculations, and these calculations, assuming rapid X state repopulation, would be approached in a solvent in which vibrational relaxation were slow. The absorption kinetics following 532 nm excitation of $I_2/CFCl_3$ solutions are shown in Fig. 6. The data is qualitatively similar to that obtained in I_2/CCl_4. Data taken at slower streak rates indicate a 2.3 ns A' state lifetime. There are, however, several important differences between the kinetics obtained in these solvents. The 580 and 640 nm short lived residual absorption maxima shown in Fig. 7 occur at 240 and 160 ps, respectively. This is considerably later than the 130 and 100 ps obtained in CCl_4 indicating slower vibrational relaxation in $CFCl_3$. Consistent with these kinetics, the fast component of the bleach recovery has a "half-life" of 280 ps in $CFCl_3$ compared with 140 ps in CCl_4. As expected, the lower rate of vibrational relaxation results in smaller discrepancies between the experimental residual absorbances and the curves calculated assuming rapid X state repopulation [Fig. 7(a)] than in the CCl_4 case [Fig. 5(a)]. However, as in the CCl_4 case, the data can be accurately simulated only if the assumption of rapid X state repopulation is removed. The calculations very accurately reproduce the experimental kinetics with a 55 ps X state repopulation lifetime [Fig. 7(b)]. The $\sim$15 ps B state predissociation lifetime indicates that, just as for CCl_4, there is a 40 ps average lifetime for atoms to repopulate the X state. In accord with the slower rate of vibrational relaxation indicated by later times at which the 580 and 640 nm absorptions are at their maxima, a $P(0,1)$ of 1/570 was used in the calculations in Fig. 7(b). This indicates that vibrational relaxation in $CFCl_3$ is a factor of $\sim$2.7 slower than in CCl_4.

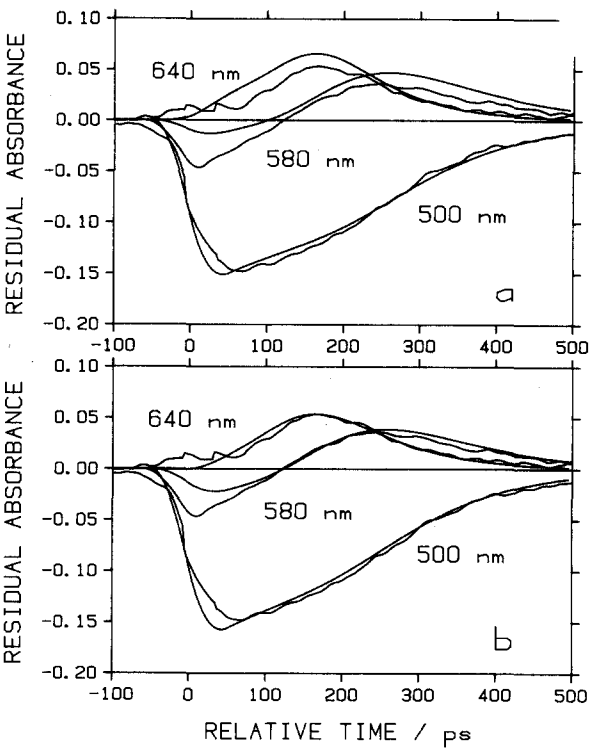

FIG. 7. Analogous plots to those in Fig. 5, except with $CFCl_3$ solvent. The calculated curves correspond to (a) $Z_{10} = 690$, $\tau_x = 15$ ps and (b) $Z_{10} = 570$, $\tau_x = 55$ ps.

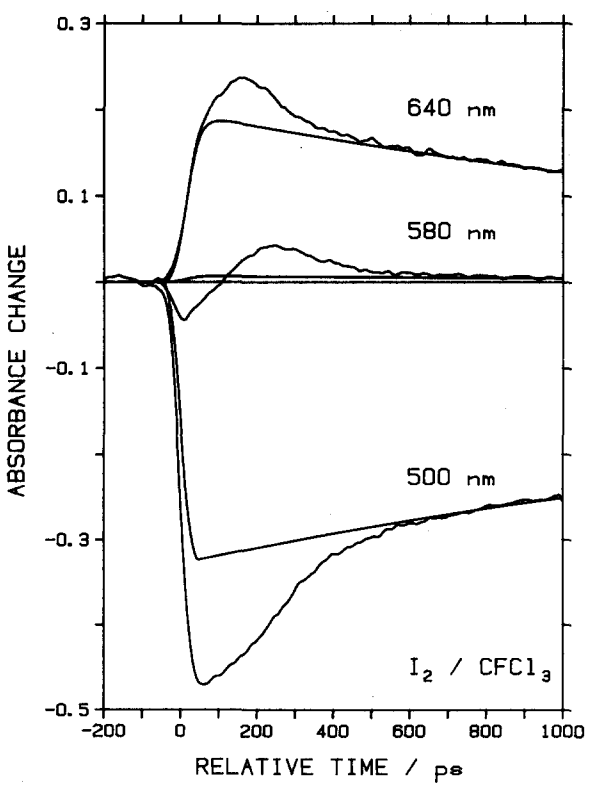

FIG. 6. Analogous plots to those in Fig. 3, except with $CFCl_3$ solvent. The calculated curves have a 2.3 ns time constant.

As discussed above, the relative values of X state repopulation and vibrational relaxation times determine the amplitudes of the 640 and 580 nm short lived residual absorbances. The maxima of the 580 and 640 nm transients, when normalized to the maximum 500 nm residual absorbance are therefore a measure of the relative rates of X state repopulation and vibrational relaxation. These $A(580)/A(500)$ and $A(640)/A(500)$ values will approach those calculated assuming prompt X state repopulation when the repopulation time is negligible compared to the relaxation time. These values for several solvents are summarized in Table I.

Figures 3 and 6 show that the 640 nm absorption from the $A'(^3\pi_{2u})$ appears rapidly following dissociation. Based on these results and those obtained in rare gas matrices,[20,21] we predict that recombination must also occur onto the slightly higher energy $A(^3\pi_{1u})$ state. However, no slow increase in A' state absorption associated with A to A' relaxation is observed. We conclude that the A and A' states are populated and equilibrate rapidly following dissociation. The above discussion raises questions regarding the mechanism of slow (tens of picoseconds) X state repopulation.

TABLE I. Summary of the vibrational relaxation and X state repopulation kinetics for iodine in various solvents. All times are in picoseconds.

Solvent	$\tau_{max}(640)$	$\tau_{max}(580)$	$A(640)/A(500)$	$A(580)/A(500)$	$T_{1/2}(500)$	Z_{10}[a]	τ_x[b]	λ_{max}/nm
$CFCl_3$	160	240	0.36	0.24	280	570	55	519
$C_2Cl_3F_3$	100	150	0.30	0.20	160	280	55	519
CCl_4	100	130	0.23	0.13	140	210	55	516
$CHCl_3$	85	130	0.31	0.23	120	c	c	511
CH_2Cl_2	40	60	0.15	0.14	95	c	c	504
Calculation ($Z_{10}=500$ $\tau_x=0$)	115	185	0.48	0.305	230	500	0	

[a] Average number of collisions required for a $v=1$ to $v=0$ transition.
[b] Average X state repopulation time. This includes the ~ 15 ps B state predissociation lifetime.
[c] SSH theory is not applicable to relaxation in these solvents (see the text).

Two mechanisms of producing a significant fraction of slow X state repopulation can be suggested:

There are several other very weakly bound electronic states upon which recombination can occur. Specifically, calculations have indicated that the $^3\pi_{0^-_u}$ state has a dissociated energy of several hundred wave numbers.[27,35] This or perhaps several other states could provide very shallow traps which relax to the X state on the tens of picoseconds time scale. The fact that most, if not all, A and A' state population occurs promptly following dissociation is perhaps somewhat difficult to explain in terms of a shallow trap model. Atom recombination following dissociation appears to populate both A' and X states. Based upon this observation, one would predict that relaxation from a shallow trap would populate the A and A' states, as well as the X state. This would lead to a slowly appearing component of the A' state absorption, contrary to the experimental observations. However, the relative rates of collisionally induced curve hopping from states such as the $^3\pi_{0^-_u}$ to the A, A', and X states are determined by the crossings and interactions of these states at large internuclear separations. The details of these interactions are unknown and may also depend upon the solvent environment. Therefore, one cannot exclude the shallow trap explanation based on this argument. Moreover, recombination into other electronically excited states (specifically the A' state) supports the plausibility of this explanation. Clearly, a detailed theoretical analysis would be helpful in resolving this issue.

The other possible mechanism by which slow X state repopulation might occur is slow atom recombination. This explanation depends crucially upon the distribution of internuclear separations obtained following dissociation. In this model, those atoms ($\sim 17\%$ in CCl_4 following B state excitation) which obtain quite large internuclear separation will have a high probability of cage escape. The atoms which obtain relatively small internuclear separations will recombine quite rapidly. This recombination would be partitioned between the electronically excited states and the X state. As shown by Ali and Miller,[24] at very small internuclear separations level hopping from the dissociative state to the electronically excited states is favored due to the the large energy gap to the X state. At somewhat larger internuclear separations level hopping and hence recombination on the X state will be favored. The fairly small fraction of atoms that obtain these intermediate internuclear separations are therefore expected to favor recombination on the X state. It is possible that these atoms will recombine on a tens of picoseconds time scale.

The time scale of radical pair geminate recombination may be relevent to this discussion.[28] Photolysis of 1,3-diphenyl acetone in organic solvents is known to produce triplet benzyl radical pairs. Geminate recombination can occur only following intersystem crossing to the singlet surface. ESR and isotope data indicates that intersystem crossing occurs on the nanosecond time scale. However, the geminate recombination quantum yield is 5%–10%, indicating that geminate recombination occurs on the 100 ps time scale. This reaction is discussed in detail in Ref. 28 (b). While no direct comparison between the radical pair studies and the present work can be made, the radical pair studies do suggest that a ~ 50 ps time scale for atom recombination is not unreasonable.

The plausibility of this mechanism has been extensively addressed in theoretical studies.[10–18] The consensus from the molecular dynamics, generalized Langevin, and molecular time scale generalized Langevin studies is that all atom recombination occurs very rapidly (<20 ps). However, most of these calculations have considered only the ground electronic state. It is quite possible that inclusion of other electronic states could alter the results.

We emphasize that the experimental results reported here do not permit us to determine if trapping in shallow electronic states or slow atom recombination is responsible for the slow component of X state repopulation. Temperature dependence studies are currently in progress, and may help to resolve this ambiguity.

Vibrational relaxation rates

The results shown in Figs. 5 and 7 indicate that an isolated binary collision model such as SSH theory works quite well for I_2 in solvents such as $CFCl_3$ and CCl_4. Similar results were obtained in $C_2F_3Cl_3$ (1,1,2 trichlorotrifluoroethane). The kinetics obtained for I_2/CH_2Cl_2 are shown in Figs. 8 and 9. These figures and Table I show that the 640 and 580 nm maximum absorbances occur 45 and 60 ps following excitation. This is close to being limited by the 35 ps FWHM instrument response function and we conclude that vibra-

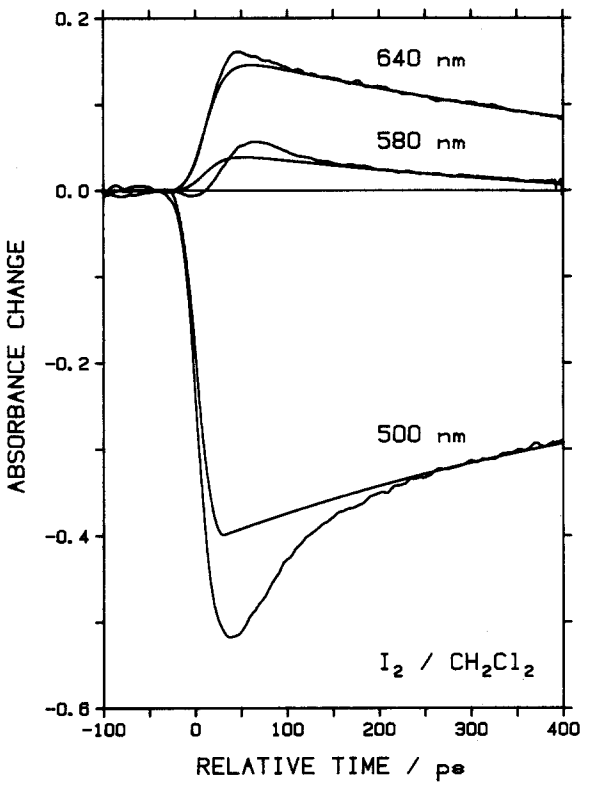

FIG. 8. Analogous plots to those in Fig. 3, except with CH_2Cl_2 solvent. The calculated curves have a 600 ps time constant.

tional relaxation occurs very rapidly in this solvent. This conclusion is further supported by the ratios of maximum absorbances at 580 compared to 500 nm and 640 compared to 500 nm given in Table I. These ratios are much smaller than those obtained in CCl_4, $C_2F_3Cl_3$, or $CFCl_3$, indicating that, unlike these solvents, vibrational relaxation in CH_2Cl_2 is quite fast compared to X state repopulation. The relative magnitudes of the $A(580)/A(500)$ and $A(640)/A(500)$ ratios are also significantly different from those obtained in CCl_4, $C_2F_3Cl_3$, or $CFCl_3$. Table I shows that the amplitude of the 640 nm transient was considerably larger than that obtained at 580 nm in CCl_4, $C_2F_3Cl_3$, and $CFCl_3$. However, they are of comparable amplitude in CH_2Cl_2. While the entire vibrational relaxation process is considerably faster than in the other solvents, this result indicates that in CH_2Cl_2 there is very rapid relaxation in the upper vibrational levels followed by relative stagnation in the lower vibrational levels. This effect is much more pronounced than predicted by the SSH theory calculation, resulting in the anomolously weak 640 nm transient. We are therefore unable to simultaneously fit curves calculated by SSH theory to the 500, 580, and 640 nm CH_2Cl_2 experimental data. The same was found to be true with $CHCl_3$, but to a smaller extent. The reason why SSH theory works well in CCl_4, $CFCl_3$, and $C_2Cl_3F_3$, but breaks down in CH_2Cl_2 and $CHCl_3$ may be understood in terms of the extent of I_2–solvent interactions. The extent to which the I_2 static absorption maxima are shifted to the blue is a measure of the strength of I_2–solvent interaction.[36] The static gas phase absorption spectrum has its maximum at 526 nm. Table I shows that CH_2Cl_2 and $CHCl_3$ produce the largest perturbations while $CFCl_3$ and $C_2F_3Cl_3$ produce the smallest perturbations of the static iodine spectrum. We note that CH_2Cl_2 and $CHCl_3$ have the lowest ionization potentials of these solvents, implying that charge transfer interactions may be quite important. Table I also shows that those solvents which perturb the spectrum the least (and therefore have the weakest I_2–solvent interaction strengths) undergo the slowest vibrational relaxation.

Transient vibrational population distributions calculated for I_2 in CCl_4 are shown in Fig. 10. These populations correspond to the absorption kinetics shown in Fig. 5(b). Figure 10 shows rapid relaxation in the upper vibrational levels followed by stagnation in the lower levels as predicted by SSH theory. Qualitatively similar distributions were obtained in other weakly interacting solvents such as $CFCl_3$ and $C_2Cl_3F_3$.

It is interesting to note that vibrational relaxation occurs more rapidly in CH_2Cl_2 than in CCl_4. The lowest vibrational frequency of CCl_4 closely matches the I_2 vibrational frequency. Resonant vibration to vibration energy transfer might therefore be expected to be quite efficient in CCl_4. No

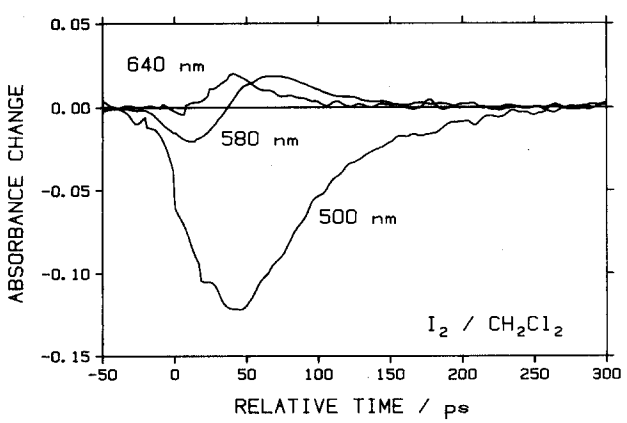

FIG. 9. Analogous plots to those in Fig. 5, except with CH_2Cl_2 solvent. No calculated curves are shown (see the text).

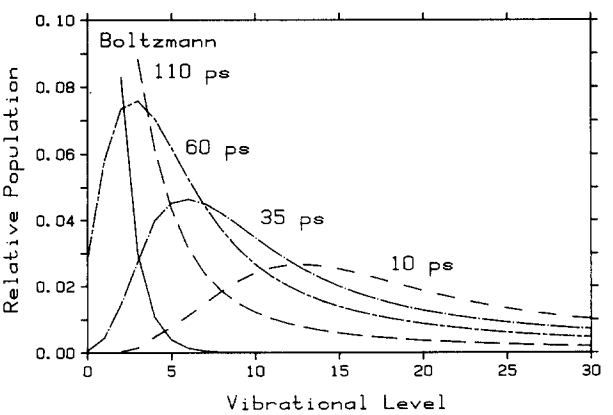

FIG. 10. Calculated plots of the time depenent X state vibrational populations of I_2 in CCl_4. These population distributions correspond to the transient absorption kinetics shown in Fig. 5(b). The solid curve corresponds to a Boltzmann distribution.

such frequency match exists for I_2 in CH_2Cl_2 and vibration to vibration (V–V) energy transfer is expected to be inefficient. Faster relaxation in CH_2Cl_2 does not preclude the possibility that (V–V) energy transfer has some role in the relaxation process. However, this result, and the accuracy with which a pure vibration to translation (V–T) isolated binary collision model fits the experimental results indicates that V–T energy transfer is the primary relaxation mechanism. Futhermore, the solvent studies show that the relaxation rate is primarily determined by the strength of the I_2–solvent interaction.

It is of interest to compare the I_2/CCl_4 vibrational relaxation rates to those obtained Br_2/CCl_4 (Ref. 37). Ultrasonic data indicates that the V–T relaxation in bromine is about an order of magnitude slower than it is iodine.[32,34] However, picosecond spectroscopic studies of Br_2/CCl_4 reported in Ref. 37 show that the vibrational relaxation is slightly faster than the I_2/CCl_4 relaxation reported here. The 500 nm kinetic data in Ref. 37 indicate a bromine bleach recovery "half-life" of about 100 ps, compared with the iodine value of 140 ps reported here. The observed differences in relaxation rates may be understood in terms of the CCl_4 normal modes, and the role of V–V energy transfer. As indicated above, the 214 cm^{-1} I_2 stretching frequency is nearly resonant with the 218 cm^{-1} lowest doubly degerate bending mode of CCl_4. However, this bending mode is orthogonal and therefore uncoupled to the I_2 stretch in a direct end on collision.[38] Other collision geometries are also expected to be inefficient because CCl_4 is approximately spherical in a low energy collision with a large partner. The Br_2/CCl_4 vibrational coupling is much different than in the I_2/CCl_4 case. The 325 cm^{-1} Br_2 stretch is nearly resonant with the triply degenerate 314 cm^{-1} "distortion" mode of CCl_4. Oscillation of this normal mode changes bond angles and C–Cl bond lengths.[38] The Br_2 stretch is therefore coupled to this mode in a direct, end on collision. We conclude that Br_2 but not I_2 in CCl_4 vibrationally relaxes primarily via a V–V energy transfer mechanism.

Excitation at 630 and 683 nm

The iodine dissociation and recombination dynamics can be further studied by variation of the excitation energy. Excitation at 532 nm predominately populates the $B(^3\pi_0)$ state. This state rapidly predissociates onto a repulsive surface resulting in 3220 to about 4000 cm^{-1} of excess energy. The former value assumes that B state vibrational relaxation is complete prior to predissociation. Alternatively, 630 and 683 nm excitation populates dissociative levels of the $A(^3\pi_{1u})$ state, resulting in about 3330 and 2090 cm^{-1} of excess energy, respectively. It is expected that these differences in the dissociative potential surface and recoil energy could affect the recombination dynamics, and therefore alter the branching ratios for excited and ground state recombination and cage escape. The branching ratios are expected to be excitation wavelength dependent partially for the same reason that they are strongly solvent dependent.[25] In less viscous solvents the recoiling atoms attain larger internuclear separations and are therefore more likely to escape the solvent cage. Furthermore, at smaller internuclear separations level hopping is facile only to weakly bound states including the A and A' states, and their population is favored in more viscous solvents. Clearly, solvent characteristics other than the viscosity must be involved in the determination of the branching ratios, but a reasonable correlation with viscosity has been obtained.[25] The distribution of internuclear separations attained upon dissociation should also depend upon the nature of the dissociative surface and/or the recoil energy. One expects that dissociation on a purely repulsive surface will result in larger internuclear separations than would be obtained from dissociative levels of the weakly bound $A(^3\pi_{1u})$ surface. Furthermore, it is expected that $A(^3\pi_{1u})$ state excitation may favor recombination on that same state. The branching ratios obtained in CCl_4 and CH_2Cl_2 solvents are given in Table II. Excitation with 683 and 630 nm light results in virtually identical branching ratios in both CCl_4 and CH_2Cl_2 solvents. This indicates that changing the recoil energy from 2090 and 3330 cm^{-1} has a negligible effect on the recombination dynamics. B state (532 nm) predissociation results in roughly the same recoil energy as 630 nm excitation. However, dissociation on a purely repulsive surface results in a larger fraction of cage escape and a smaller fraction of excited state recombination. We conclude that within the range of energies studied here, it is the nature of the dissociative surface, not the recoil energy which primarily determines the recombination dynamics.

Only very slight changes in the fast component of the bleach recovery kinetics were observed following 683 compared to 532 nm excitation, and may be due to the absence of B state predissociation in the 683 nm case. This is consistent with the above interpretations: The time required for this recombination to occur depends primarily upon the electronic states in which trapping occurs and is independent of the dissociative state. It is expected that changes in the branching ratios for population of shallow trapping states would result in slight changes in the X state repopulation kinetics. Alternatively, changes in the distribution of internuclear separations could change the fraction of atoms at intermediate internuclear separations which undergo slow (tens of picoseconds) recombination. However, in either case, these subtle effects are very difficult to observe due to the kinetics of B state predissociation, and difficulties inherent in the measurement of transient absorption intensities.

CONCLUSIONS

(1) Ground electronic state repopulation takes place on

TABLE II. Summary of the branching ratios into the electronically excited A' state, the ground electronic state, and cage escape.

		Excitation wavelength 532 nm	630 nm	683 nm
CCl_4	A'	0.44	0.64	0.58
	X	0.39	0.32	0.37
	Esc.	0.17	0.04	0.05
CH_2Cl_2	A'	0.46	0.67	0.66
	X	0.22	0.21	0.21
	Esc.	0.32	0.12	0.13

the 30–50 ps time scale. The average X state repopulation lifetime for I_2 in CCl_4 is about 40 ps. Recombination into the electronically excited A and A' states takes place quite rapidly (<30 ps). We propose that this difference in time scales may be understood in terms of trapping in shallow electronic states (perhaps $^3\pi_{0^-_u}$) which gives rise to a significant fraction of slower X state repopulation. These kinetics may also be interpreted in terms of a component of slow atom recombination, which favors the X state.

(2) Variation of the excitation energy and therefore dissociative surface involved affects the distribution of internuclear separations obtained, and therefore the branching ratios for excited and ground state recombination, and cage escape.

(3) Vibrational relaxation in weakly interacting solvents closely follows the predictions of an isolated binary collision model (SSH theory). The main relaxation mechanism is by vibrational to translational energy transfer. Resonant vibration to vibration energy transfer in I_2/CCl_4 is relatively unimportant. This may be due to the inability of the I_2 stretch to couple to the resonant CCl_4 bending modes.

(4) Strongly interacting solvents lead to very rapid vibrational relaxation. SSH theory is not applicable to relaxation in these solvents.

ACKNOWLEDGMENTS

The authors would like to thank the donors of the Petroleum Research Fund administered by the ACS, the National Science Foundation, the Research Corporation, and IBM for support of this work. We would also like to thank Professor D. Farrelly for his help in the calculation of the Franck–Condon factors, and Professor K. B. Eisenthal for helpful discussions.

[1] J. Tellinghuisen, J. Chem. Phys. **76**, 4736 (1982), **78**, 2374 (1983), and references therein; R. S. Mulliken, *ibid.* **55**, 288 (1971).
[2] E. Rabinovitch and W. C. Wood, Trans. Faraday Soc. **32**, 1381 (1936).
[3] (a) R. M. Noyes and J. Zimmerman, J. Chem. Phys. **18**, 656 (1950), (b) R. M. Noyes, *ibid.* **22**, 1349 (1954); (c) F. W. Lampe and R. M. Noyes, J. Am. Chem. Soc. **76**, 2140 (1954); (d) R. M. Noyes, *ibid.* **77**, 2042 (1955); **78**, 5486 (1956); **81**, 566 (1959); (e) H. Rosman and R. M. Noyes, *ibid.* **80**, 2410 (1958); (f) D. Booth and R. M. Noyes, *ibid.* **82**, 1868 (1960); (g) L. F. Meadows and R. M. Noyes, *ibid.* **82**, 1872 (1960); (h) R. M. Noyes, Z. Elektrochem. **64**, 153 (1960).
[4] K. Luther and J. Troe, Chem. Phys. Lett. **24**, 85 (1974).
[5] J. C. Dutol, J. M. Zellweger, and H. van den Bergh, J. Chem. Phys. **78**, 1825 (1982).
[6] T. J. Chuang, G. W. Hoffman, and K. B. Eisenthal, Chem. Phys. Lett. **25**, 201 (1974).
[7] K. Huber and G. Herzberg, *Constants of Diatomic Molecules* (Van Nostrand Reinhold, New York, 1979), and references therein.
[8] (a) C. A. Langhoff, B. Moore, and M. DeMeuse, J. Am. Chem. Soc. **104**, 3576 (1982); (b) J. Chem. Phys. **78**, 1191 (1983).
[9] D. F. Kelley and P. M. Rentzepis, Chem. Phys. Lett. **85**, 85 (1982).
[10] (a) P. Bado, P. H. Berens, and K. R. Wilson, Proc. Soc. Photo-Op. Instrum. Eng. **322**, 230 (1982); (b) P. Bado, P. H. Berens, J. P. Bergsma, S. B. Wilson, and K. R. Wilson, in *Picosecond Phenomena III*, edited by K. B. Eisenthal, R. M. Hochstrasser, W. Kaiser, and A. Laubereau (Springer, Berlin, 1982), p. 260.
[11] S. H. Northrup and J. T. Hynes, J. Chem. Phys. **71**, 871, 884 (1979).
[12] J. T. Hynes, R. Kapral, and G. M. Torrie, J. Chem. Phys. **72**, 177 (1980).
[13] J. N. Murrel, A. J. Stace, and R. Dammel, J. Chem. Soc. Faraday Trans. 2 **74**, 1532 (1978).
[14] B. Martire and R. G. Gilbert, Chem. Phys. **56**, 241 (1981).
[15] (a) C. L. Brooks III, M. W. Balk, and S. A. Adelman, J. Chem. Phys. **79**, 784 (1983); (b) M. W. Balk, C. L. Brooks, and S. A. Adelman, *ibid.* **79**, 804 (1983).
[16] M. Schell and Kapral, Chem. Phys. Lett. **81**, 83 (1981).
[17] K. J. Shin and R. Kapral, J. Chem. Phys. **69**, 3685 (1978).
[18] D. J. Nesbitt and J. T. Hynes, J. Chem. Phys. **77**, 2130 (1982).
[19] P. Bado, C. Dupuy, D. Madge, K. R. Wilson, and M. Malloy, J. Chem. Phys. **80**, 5531 (1984).
[20] M. L. Mandich, P. B. Beeken, and G. Flynn, J. Chem. Phys. **77**, 702 (1982).
[21] P. B. Beeken, M. L. Mandich, and G. Flynn, J. Chem. Phys. **76**, 5995 (1982).
[22] V. E. Bondybey and C. Fletcher, J. Chem. Phys. **64**, 3615 (1976).
[23] V. E. Bondybey, S. S. Bearder, and C. Fletcher, J. Chem. Phys. **64**, 5243 (1976).
[24] (a) D. P. Ali and W. H. Miller, J. Chem. Phys. **78**, 6640 (1983); (b) Chem. Phys. Lett. **105**, 501 (1984).
[25] (a) D. F. Kelley, N. A. Abul-Haj, and D. J. Jang, J. Chem. Phys. **80**, 4105 (1984); (b) D. F. Kelley and N. A. Abul-Haj, in *Ultrafast Phenomena IV*, edited by K. B. Eisenthal (Springer, Berlin, 1984), p. 292; (c) Proc. SPIE-Int. Soc. Photo-Opt. Eng. **533**, 20 (1985).
[26] (a) M. Berg, A. L. Harris, J. K. Brown, and C. B. Harris in Ref. 25(b), p. 300; (b) Phys. Rev. Lett. **54**, 951 (1985).
[27] J. M. Dawes and M. G. Sceats, Chem. Phys. **96**, 315 (1985).
[28] (a) G. L. Closs, R. J. Miller, and O. D. Redwing, Acc. Chem. Res. **18**, 196 (1985); (b) N. J. Turro and G. C. Weed, J. Am. Chem. Soc. **105**, 1861 (1983).
[29] D. J. Jang and D. F. Kelley, Rev. Sci. Instrum. (in press).
[30] N. A. Abul-Haj and D. F. Kelley (in preparation).
[31] M. Child, *Semiclassical Methods in Molecular Scattering and Spectroscopy* (Reidel, Dordrecht, 1980), pp. 127–154.
[32] J. D. Lambert, *Vibrational and Rotational Relaxation in Gases* (Clarendon, Oxford, 1977).
[33] R. N. Schwartz, Z. I. Slawsky, and K. F. Herzfeld, J. Chem. Phys. **20**, 1591 (1952).
[34] F. D. Shields, J. Acoust. Soc. Am. **32**, 180 (1960).
[35] E. P. Gordeev, S. Y. Umansky, and A. I. Voronin, Chem. Phys. Lett. **23**, 524 (1973).
[36] J. Yarwood, *Spectroscopy and Structure of Molecular Complexes* (Plenum, New York, 1973).
[37] N. A. Abul-Haj and D. F. Kelley, Chem. Phys. Lett. **119**, 182 (1985).
[38] G. Herzberg, *Infrared and Raman Spectra* (Van Nostrand Reinhold, New York, 1945).